

Measurements of inclusive, boson-tagged, and heavy quark flavor jet energy loss in PbPb collisions at $\sqrt{s_{NN}} = 5.02$ TeV with the CMS detector

Xiao Wang, on behalf of the CMS Collaboration*

The University of Illinois at Chicago

E-mail: x.wang@cern.ch

In this talk, we present measurements of jet energy loss in jets back-to-back with a Z or photon tag. With a clean tag of initial parton momentum quantifying the magnitude of energy loss, we then study the angular redistribution of energy with inclusive jet shapes, boson-tagged jet shapes. The implications of these measurements are discussed through comparisons of jet energy loss, redistribution, and the medium response as a function of the parton flavor.

*International Conference on Hard and Electromagnetic Probes of High-Energy Nuclear Collisions
30 September - 5 October 2018
Aix-Les-Bains, Savoie, France*

*Speaker.

1. Introduction

After jet quenching was observed in several studies at RHIC [1] and LHC [2], jets, as objects closely related to the parton created in the initial hard scattering can be good probes to study the parton energy loss while traversing the hot median. Furthermore, various types of jets may advance the study of energy loss from different aspects. Z boson and photons do not carry color charge and therefore do not interact with the QGP. These color neutral objects can be used to control the initial state of the hard process in the collision to provide a reference to the recoiling jet. Although the cross-section of Z bosons are smaller than that of the photons, the Z boson selection is affected to a lesser extent by contamination compared to the photon selection.

On the other hand, the jet quenching may depend on the type of the partons initiating the jets [3]. The jets associated with an isolated photon mainly originate from quarks [4] and therefore can be used to determine the quark and gluon behavior in the quenching by comparing it to the inclusive studies [5]. Furthermore, the b-tagging method provides a way to select the jets originated from bottom quarks, which can be used to study the jet quenching as a function of the parton flavor. CMS experiments provided a great opportunity to study on these topics [6].

2. Jet quenching in various types of jets

Figure 1 shows the photon+jet transverse momentum imbalance $X_{J\gamma} = p_T^{\text{jet}}/p_T^\gamma$ for PbPb in different centrality bins. Comparing to the pp reference overlaid, jet transverse momentum in the heavy-ion collision is shifted significantly towards low p_T implying jet suppression. The Z boson+jet X_{JZ} measurement (right canvas, Fig. 2) shows a similar level of jet transverse momentum shift compared to the pp reference. Meanwhile, no broadening is observed in the $\Delta\phi = |\phi_J - \phi_Z|$ distribution which has been normalized by the number of Z bosons (left canvas, Fig. 2).

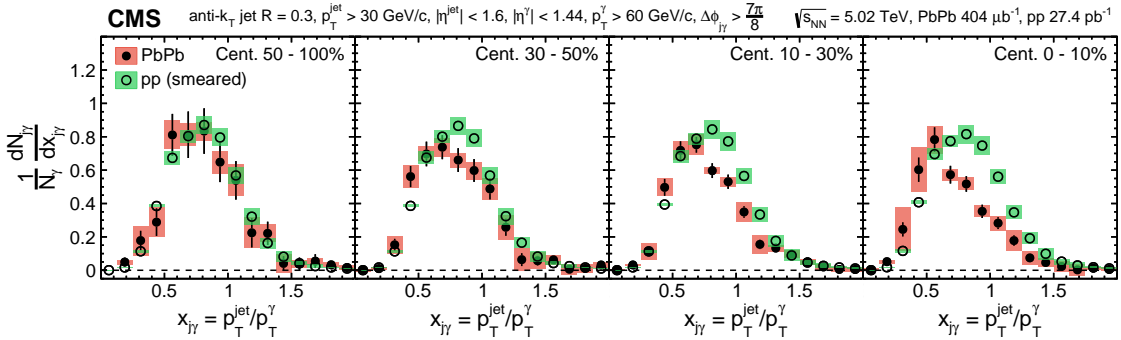


Figure 1: The centrality dependence of $X_{J\gamma}$ of photon+jet pairs normalized by the number of photons for PbPb (full markers) and smeared pp (open markers) data. The vertical lines (bands) through the points represent statistical (systematic) uncertainties [7].

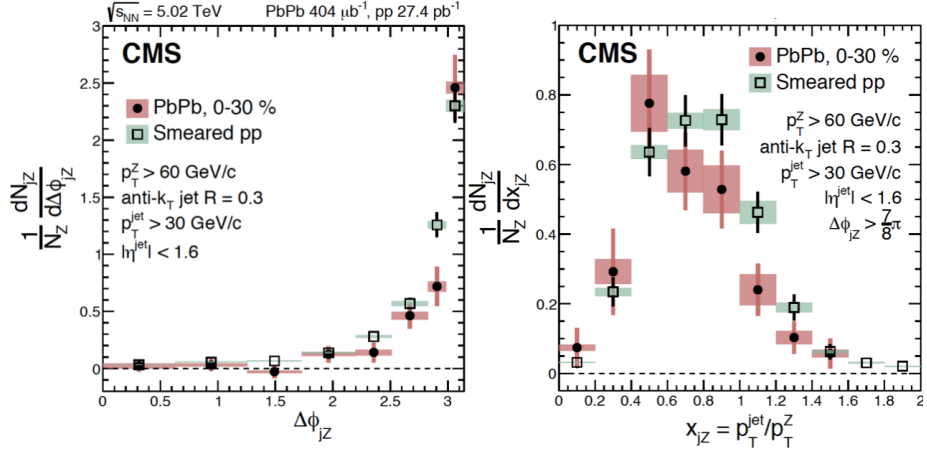


Figure 2: Distributions of the azimuthal angle difference $\Delta\phi_{JZ}$ between the Z boson and the jet (left), and of the transverse momentum ratio x_{JZ} between the jet and the Z boson with $\Delta\phi_{JZ} > 7\pi/8$ (right). The distributions are normalized by the number of Z events, N_Z . Vertical lines (bands) indicate statistical (systematic) uncertainties [8].

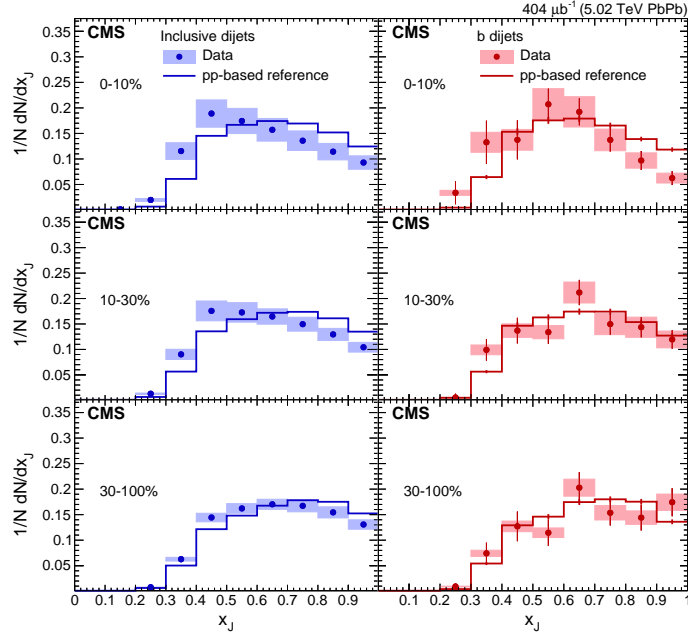


Figure 3: Distributions of X_J in PbPb collisions for inclusive dijets (left) and b dijets (right). Systematic uncertainties are shown as shaded boxes, while statistical uncertainties are shown as vertical lines. The top, middle and bottom rows show the 0–10, 10–30 and 30–100% centrality selections, respectively. The data are compared to a reference obtained by smearing pp according to the jet resolution for the given centrality class [12].

Figure 3 shows the dijet imbalance comparison between b-dijets and inclusive dijets. The b-jets are not only from the initial hard scattering but also significantly from the subsequent gluon

splitting process. Fortunately, this gluon splitting contribution will be suppressed in b dijet events which required two jets to be back-to-back. While the significant imbalance has observed in inclusive dijets in 30-100% bins, the momentum imbalance in b dijet is likely to be smaller than the inclusive dijets: b dijets imbalance is compatible with pp reference in peripheral bins (30-100%), lies between the pp and inclusive dijets in the 10-30% bin and significant shifted in bins 0-10%.

3. Energy distribution around jets

The track transverse momentum distribution around inclusive jets (Fig. 4) is defined as:

$$P(\Delta r) = \frac{1}{\delta r} \frac{1}{N_{\text{jets}}} \sum_{\text{jets, tracks} \in (\Delta r_a, \Delta r_b)} p_{\text{T}}^{\text{trk}}, \quad \Delta r < 1, \quad (3.1)$$

where Δr_a and Δr_b defines the angular edges of $\Delta r = \sqrt{(\Delta\phi)^2 + (\Delta\eta)^2}$ which is the angular distance between the jets and tracks. The ratio of the PbPb to pp data from three different $p_{\text{T}}^{\text{trk}}$ range shown in the bottom panel of Fig. 4. The observed high p_{T} particles depletion and soft particle yield enhancement relative to pp data is possibly due to the quenched jet recombination and the medium back reaction to the jets [9, 10, 11]. A pronounced energy redistribution from the small to large angles away from the jet axis is also observed in the most central collision.

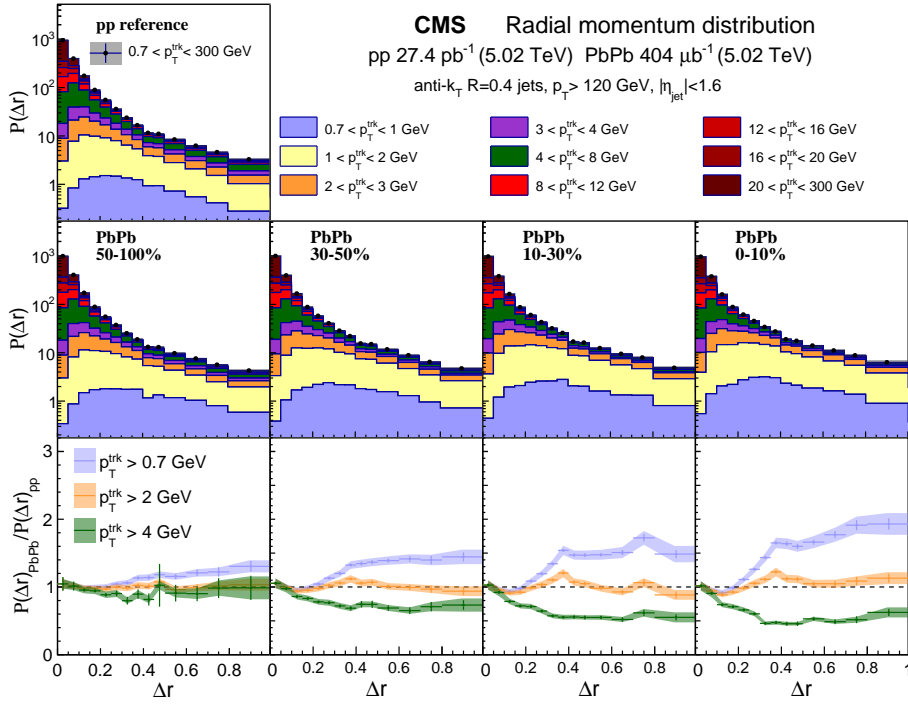


Figure 4: The distribution of jet-correlated charged-particle tracks as a function of Δr in pp (top left) and PbPb (middle row) collisions. The PbPb results are shown for different centrality regions. The bottom row shows the difference between the PbPb and pp data. The intervals in $p_{\text{T}}^{\text{trk}}$ are indicated by the stacked histograms. The inclusive points ($0.7 < p_{\text{T}}^{\text{trk}} < 20$ GeV) are shown by open white circles. The grey bands surrounding these points show the total systematic uncertainties [14].

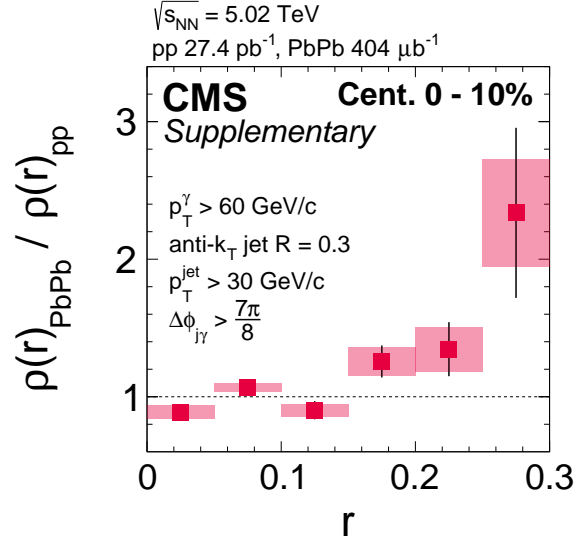


Figure 5: The ratio of PbPb over pp differential jet shape, $\rho(r)$, for 0-10% centrality interval [13].

Furthermore, the photon tagged jet shape ratio of PbPb (0–10%) to pp shown in Fig. 5 provides more constraint on the quark and gluon contribution in jet quenching as the photon tagged jets are mostly quark jets. The photon tagged jets show a similar trend in the jet shape ratio compared to the inclusive jets, except at the large r region where the former jets show a stronger enhancement.

4. Summary

CMS has measured the jet quenching and energy loss using different types of jets. The jet imbalance measurement is performed for inclusive dijets, photon+jets, Z boson+jets, and the b dijets and will put strong constraints for modeling the interaction between parton and medium. CMS also extended the measurement to other jet properties, like transverse momentum distribution and the jet shapes, for inclusive jets and photon tagged jets. It is generally observed that the high p_{T} particles around the jets are shifted to the lower p_{T} region and the energy is redistributed from small Δr region to large Δr region and this feature seems even stronger in the photon tagged jets.

References

- [1] J. Adams *et al.* [STAR Collaboration], Nucl. Phys. A **757**, 102 (2005) doi:10.1016/j.nuclphysa.2005.03.085 [nucl-ex/0501009].
- [2] S. Chatrchyan *et al.* [CMS Collaboration], Phys. Rev. C **84**, 024906 (2011) doi:10.1103/PhysRevC.84.024906 [arXiv:1102.1957 [nucl-ex]].
- [3] Y. L. Dokshitzer and D. E. Kharzeev, Phys. Lett. B **519**, 199 (2001) doi:10.1016/S0370-2693(01)01130-3 [hep-ph/0106202].
- [4] D. d’Enterria and J. Rojo, Nucl. Phys. B **860**, 311 (2012) doi:10.1016/j.nuclphysb.2012.03.003 [arXiv:1202.1762 [hep-ph]].

- [5] I. Vitev, EPJ Web Conf. **172**, 05006 (2018) doi:10.1051/epjconf/201817205006 [arXiv:1711.09905 [hep-ph]].
- [6] S. Chatrchyan *et al.* [CMS Collaboration], JINST **3**, S08004 (2008). doi:10.1088/1748-0221/3/08/S08004
- [7] A. M. Sirunyan *et al.* [CMS Collaboration], Phys. Lett. B **785**, 14 (2018) doi:10.1016/j.physletb.2018.07.061 [arXiv:1711.09738 [nucl-ex]].
- [8] A. M. Sirunyan *et al.* [CMS Collaboration], Phys. Rev. Lett. **119**, no. 8, 082301 (2017) doi:10.1103/PhysRevLett.119.082301 [arXiv:1702.01060 [nucl-ex]].
- [9] J. Casalderrey-Solana, D. Gulhan, G. Milhano, D. Pablos and K. Rajagopal, JHEP **1703** (2017) 135 doi:10.1007/JHEP03(2017)135 [arXiv:1609.05842 [hep-ph]].
- [10] Y. Tachibana, N. B. Chang and G. Y. Qin, Phys. Rev. C **95**, no. 4, 044909 (2017) doi:10.1103/PhysRevC.95.044909 [arXiv:1701.07951 [nucl-th]].
- [11] I. Vitev, S. Wicks and B. W. Zhang, JHEP **0811**, 093 (2008) doi:10.1088/1126-6708/2008/11/093 [arXiv:0810.2807 [hep-ph]].
- [12] A. M. Sirunyan *et al.* [CMS Collaboration], JHEP **1803**, 181 (2018) doi:10.1007/JHEP03(2018)181 [arXiv:1802.00707 [hep-ex]].
- [13] A. M. Sirunyan *et al.* [CMS Collaboration], [arXiv:1809.08602 [hep-ex]].
- [14] A. M. Sirunyan *et al.* [CMS Collaboration], JHEP **1805**, 006 (2018) doi:10.1007/JHEP05(2018)006 [arXiv:1803.00042 [nucl-ex]].